

pubs.acs.org/JPCL Letter

Decoupled Ion Transport in Protein-Based Solid Electrolyte through Ab Initio Calculations and Experiments

Chunhua Ying, Xuewei Fu,* Wei-Hong Zhong, and Jin Liu*



Cite This: J. Phys. Chem. Lett. 2021, 12, 9429-9435



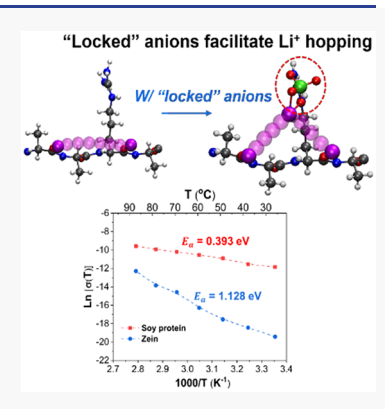
ACCESS

Metrics & More

Article Recommendations

Supporting Information

ABSTRACT: Decoupling the ion motion and segmental relaxation is significant for developing advanced solid polymer electrolytes with high ionic conductivity and high mechanical properties. Our previous work proposed a decoupled ion transport in a novel protein-based solid electrolyte. Herein, we investigate the detailed ion interaction/transport mechanisms through first-principles density functional theory (DFT) calculations in a vacuum space. Specifically, we study the important roles of charged amino acids from proteins. Our results show that the charged amino acids (*i.e.*, Arg and Lys) can strongly lock anions (ClO₄⁻). When locked at a proper position (determined from the molecular structure of amino acids), the anions can provide additional hopping sites and facilitate Li⁺ transport. The findings are supported from our experiments of two protein solid electrolytes, in which the soy protein (with plenty of charged amino acids) electrolyte shows much higher ionic conductivity and lower activation energy in comparison to the zein (lack of charged amino acids) electrolyte.



C olid polymer electrolytes (SPEs) are a promising class of electrolytes that are characterized by safety and exceptional mechanical performance compared to their liquid counterparts.^{1,2} When coupled with a lithium (Li) metal, solid-state batteries have the potential to achieve significantly higher energy density (>500 Wh/kg) in comparison to that of advanced Li-ion batteries (200-250 Wh/kg).3,4 However, unmodified SPEs such as poly(ethylene oxide) (PEO)/Li salt suffer from extremely low ionic conductivity $(10^{-7}-10^{-5})$ S/ cm) at room temperature, 5,6 which restricts them from broad applications under mild conditions. It is widely established that the ionic conductivity is determined by the density of mobile Li⁺ in a polymer matrix. The mobility of Li⁺ is associated with the continuous coordination/decoordination between the ions and the polar groups of the polymer, along with the segmental motions.8 Therefore, the core strategy to increase the ionic conductivity is to create more amorphous phase above the glass transition temperature to promote the migration of Li⁺, but unfortunately, this strategy deteriorates the mechanical strength and results in hazards such as short circuiting. As such, decoupling the ion motion from the segmental relaxation is the key for developing advanced SPEs with both high ionic conductivity and good mechanical strength.

In recent years, a number of studies have successfully fulfilled the decoupled ion transport by developing "polymerin-salt" systems, frustrated fragile polymers, and liquid-crystalline macromolecules. In a polymer-in-salt system, an enormous quantity of Li salts dissolve in a relatively small quantity of polymers, such that the Li⁺ ions migrate independently from the surroundings. For example, a poly-(acrylonitrile)-based electrolyte with salt concentrations >60

wt % showed an obvious decoupled ion transport behavior. Another idea is that the ions can move easily in rigid polymers such as polycarbonate, polystyrene, *etc.* even though the segmental relaxation is restricted, and the decoupling degree is increased with the fragility of the polymers. In these polymer systems, the ion motion occurs in the loose structure because of the frustration in packing of rigid chains. In addition, through self-assembling of liquid crystalline molecules, anisotropic ion motion pathways have been formed to decouple the ion motion and segmental relaxation. However, the ionic conductivity of those reported electrolytes is still extremely low ($<10^{-6}$ S/cm at room temperature); therefore, new electrolyte materials with decoupled ion transport are greatly needed for achieving higher ionic conductivity.

Our previous work¹⁵ reported a novel soy protein solid electrolyte showing a high room-temperature ionic conductivity ($\sim 10^{-5}$ S/cm), an excellent modulus (~ 1 GPa), and an extremely high Li⁺ transference number (0.94). We performed molecular simulations to study the interactions between LiClO₄ and protein in solutions. We found that the anions (ClO₄⁻) were strongly adsorbed by the positively charged side groups of specific amino acids (*i.e.*, Lysine (Lys) and Arginine (Arg)) because of the electrostatic interactions; the Li⁺ was

Received: July 24, 2021
Accepted: September 20, 2021
Published: September 23, 2021





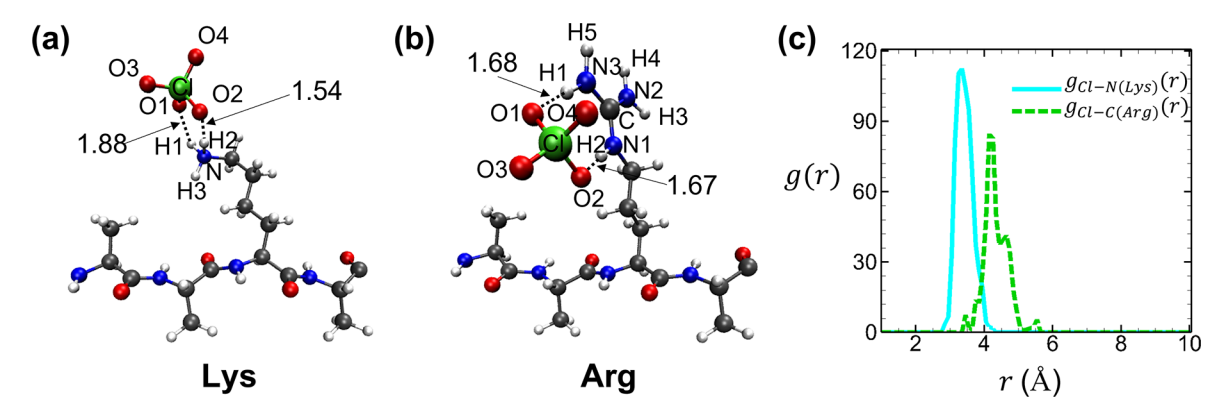


Figure 1. Fully relaxed structure of the anion and the peptide chain with different amino acid side groups in one unit cell for (a) Lys and (b) Arg. The distance of interacting hydrogen and oxygen atoms are labeled (in Å). (c) Radial distribution function between anion and the positively charged amino acid group. $g_{\text{Cl-N}(\text{Lys})}(r)$ denotes the RDF from the N atom $(-\text{NH}_3^+)$ of Lys side chain, and $g_{\text{Cl-C}(\text{Arg})}(r)$ is the RDF from the C atom $(-\text{HNC}(\text{NH}_2)_2^+)$ of Arg side chain. Cl is the chlorine atom in ClO_4^- .

Table 1. Charge Distribution of ClO₄⁻ and Positively Charged Side Groups (unit: lel)

	Lys				Arg			
[ClO ₄]	charge	[NH ₃]	charge	[ClO ₄]	charge	$[HNC(NH_2)_2]$	charge	
Cl	6.89	N1	-2.10	Cl	6.89	С	1.64	
O1	-1.96	H1	1.00	O1	-1.92	N1	-1.68	
O2	-1.91	H2	1.00	O2	-1.91	N2	-1.70	
O3	-1.96	H3	0.46	O3	-1.97	N3	-2.31	
O4	-1.92			O4	-1.95	H1	1.00	
						H2	1.00	
						H3	1.00	
						H4	0.45	
						H5	1.00	
Total	-0.86		0.36		-0.86		0.40	

less intensively adsorbed by the oxygen atoms in the protein backbones. The strength of the protein— ${\rm ClO_4}^-$ interaction and the number of adsorbed ${\rm ClO_4}^-$ were obviously increased by properly manipulating the protein structure only. Considering these findings, we proposed that in a solid protein electrolyte the backbone oxygen atoms acted as the coordinate sites for ${\rm Li^+}$ hopping while the oxygen atoms on immobilized ${\rm ClO_4}^-$ provided additional coordinate sites and facilitated the ${\rm Li^+}$ hopping. Interestingly, this hopping mode is not only different from the classic coupled ion transport in polymers but also enlightens a new and positive role from the anions. However, the simulations were performed in a solution state, and direct evidence for the ion transport in solid electrolytes is missing.

In the current work, we use first-principles density functional theory with the climbing image nudged elastic band (CI-NEB) method¹⁶ to explore the atomic-level ion transport mechanism in the protein electrolyte in a vacuum space (see the Supporting Information for computational details). Also, the density functional theory and the ab initio molecular dynamics (AIMD) simulations were performed to study the electrostatic interactions between anions and the positively charged amino acids. Although these kinds of calculations have been broadly applied to investigate the ion diffusion of solid organic or inorganic electrolytes such as PEO, Li₂S-P₂S₅ glass, solid-electrolyte interface, *etc.*, ¹⁷⁻²¹ the ion diffusion mechanisms in a protein have not been explored before. We design two short peptide chains based on two positively charged amino acids (Lys and Arg) to study the interactions with ions. Both Lys and Arg are broadly present in soy protein. The results show that both Lys and Arg peptide chains have greater binding

energies with ${\rm ClO_4}^-$ than ${\rm Li}^+$ in a vacuum space, indicating the capability of the peptides for immobilizing the anions. More significantly, ${\rm ClO_4}^-$ is steadily "locked" by the Arg peptide chain with a proper distance to the backbone and provides favorable intermediate hopping sites. As a result, the energy barrier for ${\rm Li}^+$ diffusion is significantly reduced from 0.74 to 0.37 eV. In contrast, for Lys peptides the energy barrier remains nearly unchanged because of the longer distance between "locked" ${\rm ClO_4}^-$ and the backbone. The results demonstrate that both the charge and structure of protein amino acids play important roles in locking the anions, decoupling the ${\rm Li}^+$ hopping from the segmental motion, and promoting ${\rm Li}^+$ transport.

According to our previous work, 15 the Li⁺ transference number of the soy protein electrolyte was determined to be 0.94; the MD simulation in solution indicated that the positively charged amino acids, Lys and Arg, may provide attraction to anions (ClO₄⁻). In this study, we design two peptide chains using these two amino acids as the building blocks as described in the computational methods. It is noted that Histidine (His) is not studied here because of its trivial content in the soy protein, even though it is also positively charged. 15 The ionic interactions were investigated by both DFT calculation and AIMD simulations based on a model system consisting of one peptide chain and one free anion close to the positively charged group in a vacuum space. The DFT fully relaxed constructed models are shown in Figure 1a,b. Two bonds are generated between the oxygen atoms from ClO₄⁻ and hydrogen atoms from the positively charged side groups, i.e., O1...H1 and O2...H2 bonds, the pairwise

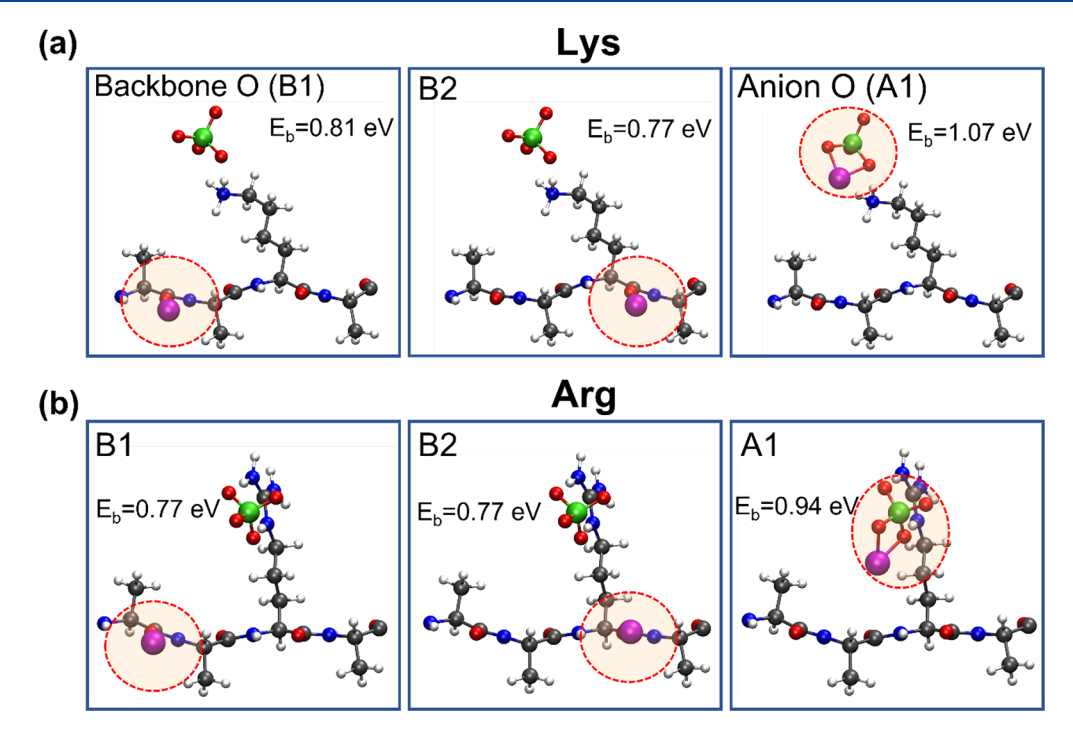


Figure 2. Top view of the different Li⁺ binding positions and the corresponding binding energy, E_{br} for (a) Lys and (b) Arg.

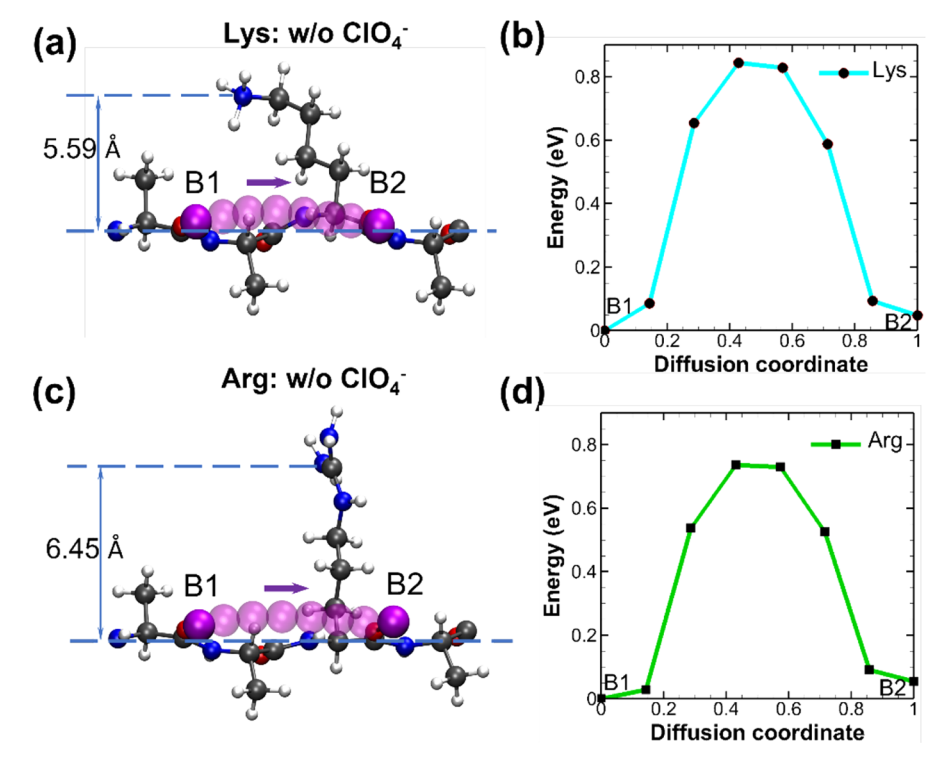


Figure 3. (a) Optimized Li⁺ diffusion pathway without anion for Lys peptide and (b) the energy profile associated with Li⁺ diffusion; (c) optimized Li⁺ diffusion pathway without anion for Arg peptide and (d) the energy profile associated with Li⁺ diffusion. The distances of the functional group to the backbone are also shown, which are calculated from the coordinates of the nitrogen atom of the -NH₃⁺ group and carbon atom of -HNC(NH₂)₂⁺ to the averaged fitted line of all the backbone atoms. Note that only the Li⁺ trajectories are shown.

distance of which are labeled alongside. The unequal bond lengths for the Lys peptides in Figure 1a are because the nitrogen atom and hydrogen atom at the end of the R group tend to have a straight lineup with the oxygen atom. The charge distribution of each atom in the entire system is calculated by Bader analysis²² as shown in Table 1. The binding hydrogen atoms, namely, H1 and H2, are polarized to

be -1.00 lel charged. The total charges for ${\rm ClO_4}^-$ in Lys and Arg systems are both -0.86 lel. Both Lys and Arg have positively charged side groups; the total charges for ε -amino group $(-{\rm NH_3}^+)$ of Lys and guanidino group $(-{\rm HNC}({\rm NH_2})_2^+)$ of Arg are 0.36 and 0.40 lel, respectively. The charge values are smaller than 1.00 lel, because they are not fully polarized in the vacuum space.

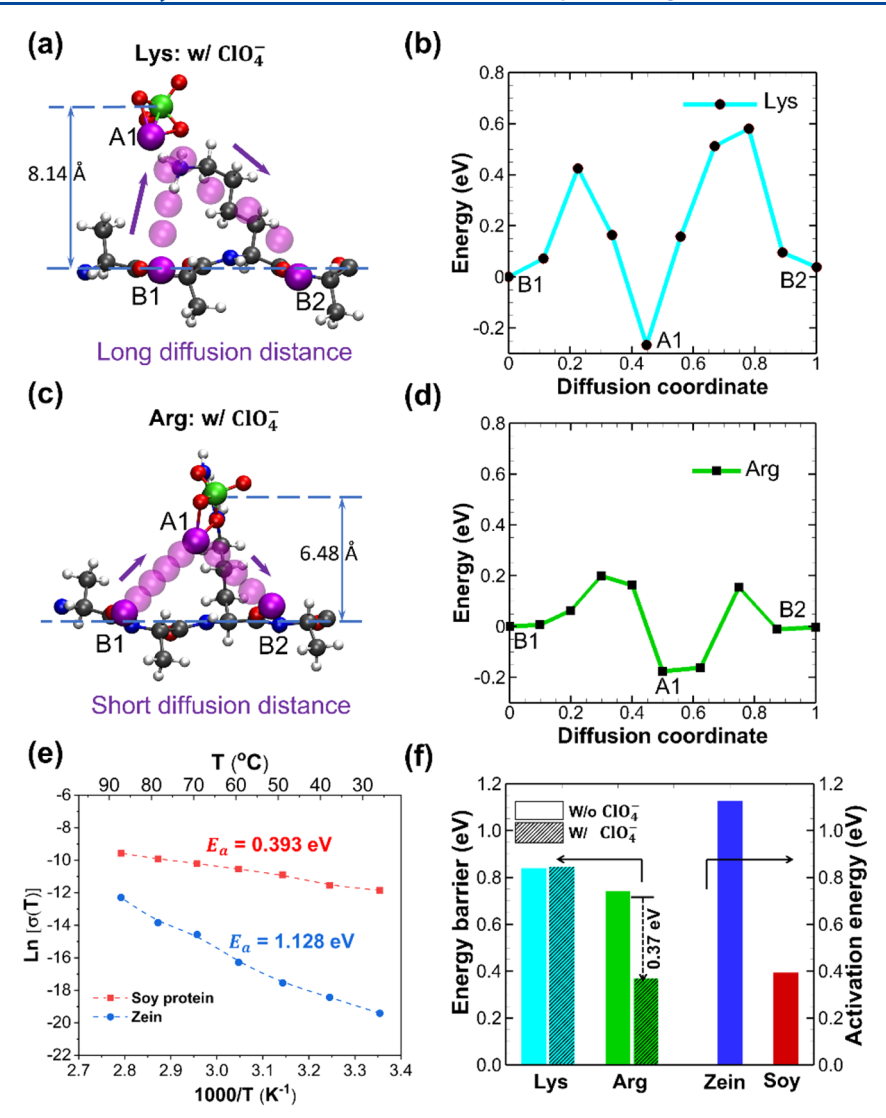


Figure 4. (a) Optimized Li⁺ diffusion pathway in Lys peptides with the $-NH_3^+$ group. The distance between the anion and the peptide backbone is shown, which is calculated by the coordinates of chlorine atom to the averaged fitted line of all the backbone atoms. (b) Energy profile for the Li⁺ diffusion along the B1-A1-B2 pathway. (c) Optimized Li⁺ diffusion pathway in Arg peptides. (d) Energy profile for the Li⁺ diffusion along the B1-A1-B2 pathway. (e) Experimental measurements of ionic conductivity at different temperatures for soy protein and zein protein-based solid electrolytes. The activation energies are calculated from the Arrhenius equation. (f) Comparison of the calculated energy barriers for the two peptides (Lys and Arg) with or without the ClO_4^- anion, the activation energies from experiments are also included for comparison.

The AIMD simulations were carried out by using the fully relaxed structure. The results show that there exists a stable interaction between ClO₄⁻ and the positively charged group in vacuum at 333 K. Figure 1c shows the radial distribution functions (RDFs) of the chlorine atom of ClO₄⁻ from the N atom of ε -amino group and C atom of the guanidino group. The r value at the RDF peak indicates the statistical stable distance. For the Lys case, the statistical stable distance between the chlorine atom of ClO₄⁻ and the nitrogen atom of the $-NH_3^+$ group is ~ 3.4 Å; this result is very close to the one obtained in a water environment by Willow and Xantheas.²³ For Arg, the statistical stable distance between the chlorine atom of ClO_4^- and carbon atom of the $-HNC(NH_2)_2^+$ group lies at ~4.1 Å. Figure 1c also shows that Lys has a higher maximum height of RDF than Arg, indicating a stronger ionic interaction between ${\rm ClO_4}^-$ and the $-{\rm NH_3}^+$ group. This is because the ε -amino group has a smaller size and has geometry more like that of sphere, while the guanidino group is known to have a wider and planar structure which may cause the

positive charge to be not as concentrated as the ε -amino group. The ionic interaction energies for the ε -amino group and guanidino group with respect to the anion are 2.73 and 2.58 eV, respectively. These results all indicate that the ε -amino group has a stronger ionic interaction with ClO_4^- .

To probe the Li⁺ binding sites of the two peptides, we perform a series of structural relaxations by randomly selecting the initial positions of Li⁺ along the peptide chains. The results show that Li⁺ is always attracted by oxygen atoms in the peptide bonds. It is known that oxygen and nitrogen atoms are likely to bind Li⁺ because they are negatively charged; however, nitrogen atoms are usually fully bonded with carbon and hydrogen, making the oxygen atoms more likely to bind Li⁺. Figure 2 shows three different Li⁺ binding positions, which are applicable for both systems: B1 and B2 represent the binding sites in the backbone oxygen atoms (only the oxygen atoms on one side of the chain are studied here, while these below the chain are similar), and A1 represents the binding sites associated with the ClO₄⁻ anion. The binding energies

(calculated from eq 1 in the Supporting Information) between Li⁺ and ClO₄⁻ (A1 site), which are 1.07 and 0.94 eV for Lys and Arg, respectively, are greater than that between Li⁺ and backbone oxygens, B1 (average 0.79 eV) and B2 sites (0.77 eV), because Li⁺ binds with two oxygen atoms of ClO₄⁻. Interestingly, if we compare with interactions between ClO₄⁻ and charged amino acids (2.73 and 2.58 eV for Lys and Arg, respectively), we find that the interaction strength is more than three times stronger. The comparison indicates that ClO₄⁻ anions can be strongly "locked" by the positively charged side groups while Li⁺ ions move more freely.

The Li⁺ diffusion pathway and the corresponding energy barrier in the absence of ClO₄⁻ are investigated by the climbing image nudged elastic band (CI-NEB) method. 16 The CI-NEB method forces the climbing image to converge to the saddle point and provides a better estimate of the energy barrier than the standard NEB method. The optimized Li+ diffusion pathways are illustrated in Figure 3a,c. As shown for both peptides, Li⁺ directly hops from B1 site to B2 site, while all the other atoms are allowed to relax near their local minimum-energy position. The corresponding energy profiles are plotted in Figure 3b,d. For both cases, each point in the plot represents an image along the diffusion pathway. In the figures, the energy (y axis) is calculated relative to the total energy of the system at the B1 site, and the diffusion coordinate (x axis) is normalized between initial position (B1 site) and final position (B2 site). The overall trend of energy profiles along the diffusion pathway is almost the same for both Lys and Arg (Figure 3b,d), because the backbone structures of the two peptide chains are identical except for the side-chain structure. However, the energy barrier for Lys (0.84 eV) is slightly greater than that of Arg (0.74 eV). This is because the -NH₃⁺ group of Lys is closer to the peptide backbone (5.59 Å) than the $-HNC(NH_2)_2^+$ group of Arg (6.45 Å), as shown in Figure 3a,c, which possibly intervenes the Li⁺ diffusion along the peptide chain. The values of the energy barrier for Li+ diffusion among backbone oxygen atoms are smaller than the values calculated for some crystalline PEO-based electrolytes (0.87-1.1 eV), $^{21,24-26}$ which indicates that the oxygen atoms on the backbone of peptides or proteins are able to act as the hopping sites for Li⁺.

When the ClO_4^- anion is introduced into the two systems, it is attracted by the positively charged groups, i.e., -NH₃⁺ and $-HNC(NH_2)_2^+$ groups. For the $-NH_3^+$ case, as shown in Figure 4a, Li⁺ first hops from B1 site to A1 site and subsequently to B2 site; the energy barrier for this diffusion pathway is 0.84 eV from the energy profile in Figure 4b. Further investigation shows that the -NH3+ group on Lys peptide may be deprotonated by the ClO₄ and Li⁺ ion pair, causing the anion to escape (see Figure S2 in the Supporting Information). In this case, Li⁺ will bind with ClO₄⁻ again. Further investigation in this respect is needed in future work. The B1-A1-B2 hopping pathway is also achieved by the Arg peptide chain as shown in Figure 4c. The energy barrier is determined to be 0.37 eV in Figure 4d, which is lower than that of the Lys peptides; the Li⁺ diffusion distance of the Lys peptides is longer than that of the Arg peptides, resulting in the higher energy barrier. More importantly, we compare the energy barriers for the cases with and without the presence of ClO₄⁻. As shown in Figure 4f, the energy barrier for Lys with or without ClO₄⁻ is identical, which is 0.84 eV. However, the energy barrier for Arg is substantially decreased from 0.74 to 0.37 eV when ClO₄⁻ is present. This suggests that a faster Li⁺

diffusion is achieved along the B1–A1–B2 pathway of the Arg case, in which the "locked" ${\rm ClO_4}^-$ provides a favorable intermediate hopping site. However, because of the greater anion–backbone distance (8.14 Å for Lys and 6.48 Å for Arg in Figure 4a,c), the B1–A1–B2 diffusion pathway is longer; as a result, we do not observe noticeable reduction of the energy barrier for the Lys case. These results indicate that the ${\rm ClO_4}^-$ residence in a proper distance to the backbone promotes the Li⁺ hopping mechanisms, decoupling the Li⁺ hopping from the segmental motion.

To verify the simulation results, we fabricate the protein-based solid electrolytes from two natural proteins: soy protein and zein (see the Supporting Information for experimental details). Soy protein has greater contents of Lys and Arg compared with zein; the contents of Lys/Arg are 6.3%/7.7% and 0.1%/1.4% for soy protein and zein, respectively. Then we measure the ionic conductivities at different temperatures; as shown in Figure 4e, the ionic conductivities are much higher for the electrolyte from soy protein. In addition, we also calculate the activation energy for ionic conduction according to the Arrhenius equation:

$$\sigma = \sigma_0 \exp(-E_a/RT) \tag{1}$$

where σ is the ionic conductivity, T is the absolute temperature, σ_0 is the pre-exponential factor, R is the gas constant, and E_a is the activation energy. By fitting the data to eq 1, the activation energy of the soy protein-based electrolyte is 0.393 eV, which is significantly lower than that of the zein-based electrolyte (1.128 eV). We compare the simulation and experiment results in Figure 4f. The activation energy from soy protein-based electrolytes is comparable to the energy barrier from the Arg case with ${\rm ClO_4}^-$. However, the activation energy of the zein protein-based electrolyte is much higher because of the lack of Arg residues. The experiment results demonstrate the importance of the positively charged amino acids to reduce the activation energy and facilitate the Li⁺ hopping.

In summary, we performed ab initio DFT calculations to explore the ion transport mechanisms in protein-based solid electrolytes. We designed two short peptides based on two positively charged amino acids (Lys and Arg) and investigated the impacts from Lys and Arg on ion interactions and diffusions. Our calculations show that the binding energy between cations (Li⁺) and backbone oxygen atoms (~0.8 eV) is similar to Li⁺-O binding in PEO-based solid electrolytes; however, the binding energy between anions (ClO₄⁻) and charged amino acids is significantly higher (~2.6-2.7 eV). The electrostatic interactions can strongly lock ClO₄-, and the immobilized ClO₄⁻ can potentially provide additional hopping sites facilitating Li+ diffusion. The structural details of the amino acids also play important roles. For example, the Arg residue is able to lock ClO₄⁻ at an appropriate position, such that the oxygen atoms from ClO₄⁻ are close to the backbone oxygen atom and provide additional hopping sites facilitating Li⁺ diffusion. This effect significantly reduces the Li⁺ diffusion energy barrier from 0.74 to 0.37 eV. However, the locked ClO₄⁻ for the Lys case is not close enough to the backbone.

The capability of charged residues to lock ClO₄⁻ to provide additional hopping sites for Li⁺ diffusion is crucial for decoupling the Li⁺ transport from segmental movements. Without sacrificing the mechanical properties, the ionic conductivity can be improved by proper design of the protein-based solid electrolytes. Moreover, the findings are also supported from our experiments by comparing the

performances of two proteins: soy protein (with plenty of charged amino acids) and zein (lacking in charged amino acids). The ionic conductivity is significantly higher and the activation energy is much lower for the soy protein-based solid electrolyte in comparison to the zein protein-based solid electrolyte. The simulations and experiments presented in this Letter yield fundamental insights on the decoupled ion transport mechanisms, and provide guidance on design and optimization for protein-based solid electrolytes with advanced performance.

ASSOCIATED CONTENT

5 Supporting Information

The Supporting Information is available free of charge at https://pubs.acs.org/doi/10.1021/acs.jpclett.1c02412.

Details of computational and experimental methods, a figure for the computational system, and a figure for fully optimized structure of deprotonated Lys peptide chain (PDF)

AUTHOR INFORMATION

Corresponding Authors

Xuewei Fu — School of Mechanical and Materials Engineering, Washington State University, Pullman, Washington 99164, United States; orcid.org/0000-0002-1164-427X; Email: xuewei.fu@wsu.edu

Jin Liu – School of Mechanical and Materials Engineering, Washington State University, Pullman, Washington 99164, United States; ⊙ orcid.org/0000-0002-0839-5153; Email: jin.liu2@wsu.edu

Authors

Chunhua Ying — School of Mechanical and Materials Engineering, Washington State University, Pullman, Washington 99164, United States

Wei-Hong Zhong — School of Mechanical and Materials Engineering, Washington State University, Pullman, Washington 99164, United States; orcid.org/0000-0002-1232-4147

Complete contact information is available at: https://pubs.acs.org/10.1021/acs.jpclett.1c02412

Notes

The authors declare no competing financial interest.

ACKNOWLEDGMENTS

The authors gratefully acknowledge the financial support by NSF CBET 1929236. Computational resources were provided in part by the Extreme Science and Engineering Discovery Environment (XSEDE) under Grant No. MCB170012.

REFERENCES

- (1) Fan, P.; Liu, H.; Marosz, V.; Samuels, N. T.; Suib, S. L.; Sun, L.; Liao, L. High Performance Composite Polymer Electrolytes for Lithium-Ion Batteries. *Adv. Funct. Mater.* **2021**, *31*, 2101380.
- (2) Choudhury, S.; Stalin, S.; Vu, D.; Warren, A.; Deng, Y.; Biswal, P.; Archer, L. A. Solid-State Polymer Electrolytes for High-Performance Lithium Metal Batteries. *Nat. Commun.* **2019**, *10*, 4398.
- (3) Albertus, P.; et al. Challenges for and Pathways toward Li-Metal-Based All-Solid-State Batteries. ACS Energy Lett. 2021, 6, 1399–1404.
- (4) Ding, Y.; Cano, Z. P.; Yu, A.; Lu, J.; Chen, Z. Automotive Li-Ion Batteries: Current Status and Future Perspectives. *Electrochem. Energy Rev.* **2019**, *2*, 1–28.

- (5) Feng, J.; Wang, L.; Chen, Y.; Wang, P.; Zhang, H.; He, X. PEO Based Polymer-Ceramic Hybrid Solid Electrolytes: A Review. *Nano Converg.* **2021**, *8*, 2.
- (6) Xue, Z.; He, D.; Xie, X. Poly(Ethylene Oxide)-Based Electrolytes for Lithium-Ion Batteries. *J. Mater. Chem. A* **2015**, *3*, 19218–19253.
- (7) Ye, F.; Liao, K.; Ran, R.; Shao, Z. Recent Advances in Filler Engineering of Polymer Electrolytes for Solid-State Li-Ion Batteries: A Review. *Energy Fuels* **2020**, *34*, 9189–9207.
- (8) Bresser, D.; Lyonnard, S.; Iojoiu, C.; Picard, L.; Passerini, S. Decoupling Segmental Relaxation and Ionic Conductivity for Lithium-Ion Polymer Electrolytes. *Mol. Syst. Des. Eng.* **2019**, *4*, 779–792.
- (9) Mackanic, D. G.; et al. Decoupling of Mechanical Properties and Ionic Conductivity in Supramolecular Lithium Ion Conductors. *Nat. Commun.* **2019**, *10*, 5384.
- (10) Forsyth, M.; Jiazeng, S.; MacFarlane, D. R. Novel High Salt Content Polymer Electrolytes Based on High Tg Polymers. *Electrochim. Acta* **2000**, 45, 1249–1254.
- (11) Agapov, A. L.; Sokolov, A. P. Decoupling Ionic Conductivity from Structural Relaxation: A Way to Solid Polymer Electrolytes? *Macromolecules* **2011**, *44*, 4410–4414.
- (12) Wang, Y.; Agapov, A. L.; Fan, F.; Hong, K.; Yu, X.; Mays, J.; Sokolov, A. P. Decoupling of Ionic Transport from Segmental Relaxation in Polymer Electrolytes. *Phys. Rev. Lett.* **2012**, *108*, 088303.
- (13) Bresser, D.; et al. Organic Liquid Crystals as Single-Ion Li⁺ Conductors. *ChemSusChem* **2021**, *14*, 655–661.
- (14) Onuma, T.; Hosono, E.; Takenouchi, M.; Sakuda, J.; Kajiyama, S.; Yoshio, M.; Kato, T. Noncovalent Approach to Liquid-Crystalline Ion Conductors: High-Rate Performances and Room-Temperature Operation for Li-Ion Batteries. *ACS Omega* **2018**, *3*, 159–166.
- (15) Fu, X.; Jewel, Y.; Wang, Y.; Liu, J.; Zhong, W.-H. Decoupled Ion Transport in a Protein-Based Solid Ion Conductor. *J. Phys. Chem. Lett.* **2016**, *7*, 4304–4310.
- (16) Henkelman, G.; Uberuaga, B. P.; Jónsson, H. A Climbing Image Nudged Elastic Band Method for Finding Saddle Points and Minimum Energy Paths. *J. Chem. Phys.* **2000**, *113*, 9901–9904.
- (17) Baba, T.; Kawamura, Y. Structure and Ionic Conductivity of Li₂S-P₂S₅ Glass Electrolytes Simulated with First-Principles Molecular Dynamics. *Front. Energy Res.* **2016**, *4*, 22.
- (18) Karmakar, S.; Chowdhury, C.; Datta, A. Two-Dimensional Group IV Monochalcogenides: Anode Materials for Li-Ion Batteries. *J. Phys. Chem. C* **2016**, 120, 14522–14530.
- (19) Lei, X.; Jee, Y.; Huang, K. Amorphous $Na_2Si_2O_5$ as a Fast Na^+ Conductor: An *Ab Initio* Molecular Dynamics Simulation. *J. Mater. Chem. A* **2015**, 3, 19920–19927.
- (20) Ramasubramanian, A.; Yurkiv, V.; Foroozan, T.; Ragone, M.; Shahbazian-Yassar, R.; Mashayek, F. Lithium Diffusion Mechanism through Solid-Electrolyte Interphase in Rechargeable Lithium Batteries. *J. Phys. Chem. C* **2019**, *123*, 10237–10245.
- (21) Xue, S.; Liu, Y.; Li, Y.; Teeters, D.; Crunkleton, D. W.; Wang, S. Diffusion of Lithium Ions in Amorphous and Crystalline Poly-(Ethylene Oxide)₃: LiCF₃SO₃ Polymer Electrolytes. *Electrochim. Acta* **2017**, 235, 122–128.
- (22) Sanville, E.; Kenny, S. D.; Smith, R.; Henkelman, G. Improved Grid-Based Algorithm for Bader Charge Allocation. *J. Comput. Chem.* **2007**, 28, 899–908.
- (23) Willow, S. Y.; Xantheas, S. S. Molecular-Level Insight of the Effect of Hofmeister Anions on the Interfacial Surface Tension of a Model Protein. *J. Phys. Chem. Lett.* **2017**, *8*, 1574–1577.
- (24) Xue, S.; Teeters, D.; Crunkleton, D. W.; Wang, S. *Ab Initio* Calculations for Crystalline PEO₆: LiPF₆ Polymer Electrolytes. *Comput. Mater. Sci.* **2019**, *160*, 173–179.
- (25) Johansson, P.; Tegenfeldt, J.; Lindgren, J. Modelling Lithium Ion Transport in Helical PEO by *Ab Initio* Calculations. *Polymer* **2001**, *42*, 6573–6577.
- (26) Karmakar, A.; Ghosh, A. Structure and Ionic Conductivity of Ionic Liquid Embedded PEO-LiCF₃SO₃ Polymer Electrolyte. *AIP Adv.* **2014**, *4*, 087112.

(27) Chen, M.; Li, C.; Fu, X.; Wei, W.; Fan, X.; Hattori, A.; Chen, Z.; Liu, J.; Zhong, W.-H. Let It Catch: A Short-Branched Protein for Efficiently Capturing Polysulfides in Lithium-Sulfur Batteries. *Adv. Energy Mater.* **2020**, *10*, 1903642.